MS-I

NASA CR-70533

ENERGY ABSORBERS

PREPARED FOR

THE GEORGE C. MARSHALL SPACE FLIGHT CENTER
NATIONAL AERONAUTICS AND SPACE ADMINISTRATION
HUNTSVILLE, ALABAMA

HAYES
INTERNATIONAL CORPORATION
BIRMINGHAM, ALABAMA

ENERGY ABSORBERS

ENGINEERING REPORT NO. 1228

21 JANUARY 1966

PREPARED FOR:

THE GEORGE C. MARSHALL SPACE FLIGHT CENTER
NATIONAL AERONAUTICS AND SPACE ADMINISTRATION
HUNTSVILLE, ALABAMA

PREPARED BY:

J. V. Hodgins

APPROVED BY:

C. L. Anker
Project Manager

P. R. Coulson
Program Manager

REVISIONS

DATE	PAGES AFFECTED	REMARKS	BY	APP.

FORM E-509 REV. 2/3/61

ABSTRACT

This report describes studies, both analytical and experimental, directed toward design of an expandable tube type tension energy absorber which maintains a constant load of 20,000 pounds throughout the stroke.

This work was performed under Contract No. NAS8-11805, for the Project Development Office, Manufacturing and Engineering Laboratory, George C. Marshall Space Flight Center, National Aeronautics and Space Administration, Huntsville, Alabama. The work was performed under the technical supervision of Mr. T. O. Eddins.

TABLE OF CONTENTS

LIST OF ILLUSTRATIONS

LIST OF TABLES

I. INTRODUCTION

There is current interest in energy absorption devices for various uses pertaining to the space program. These uses could include cushioning landing impact of vehicles, or rocket holddown releases. Various type systems have been studied, such as gas compression, material deformation, mass acceleration, friction, and retro-rockets. The most promising appears to be a system combining material deformation and friction, offering the highest energy absorption capability per unit weight of the device.

From the consideration of controllability this type of device is somewhat inferior to others, especially gas compression devices. Difficulty in controlling deceleration onset rate for a shock absorption device of this type is generally recognized.

The analytical and experimental studies described in this report were directed toward developing a means of predicting the load characteristics of an absorber of this nature. The absorber considered consists of a tube through which a mandrel is pulled, expanding the tube. Energy is absorbed through material deformation by expansion of the tube, and by friction between the mandrel and tube. The objective was to design an energy absorber of this type with a resisting load of 20,000 pounds throughout the stroke. The absorber was to be compatible with lox and to have the lightest weight possible.

II. ANALYSIS

Figure 1 shows an element of a shell of rotational symmetry being drawn over a mandrel of arbitrary shape. The forces assumed to be acting on the element are circumferential stress, longitudinal stress, mandrel pressure, and a frictional force between the shell element and the mandrel.

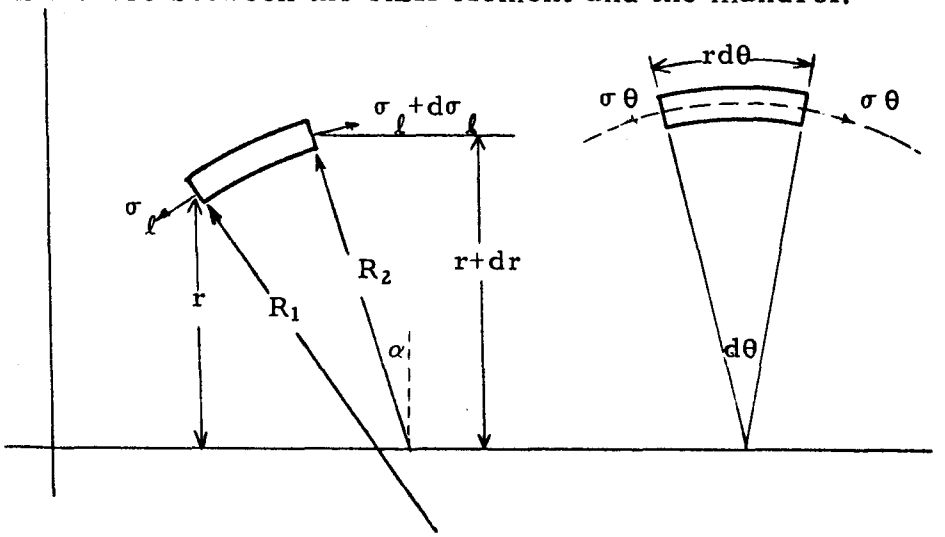

FIGURE 1 SHELL ELEMENT

Two equilibrium equations will now be written, the first with reference to the normal to the tangent plane, and the second with reference to the direction of the meridian tangent.

Equilibrium of the forces acting on the element in the direction of the normal to the tangent plane is expressed by

$$\frac{\sigma_\ell}{R_1} + \frac{\sigma_\theta}{R_2} = \frac{p}{h} \qquad (1)$$

Equilibrium in the direction of the meridian tangent is expressed by

$$\frac{d}{dr}(\sigma_\ell hr) - \sigma_\theta h - \frac{\mu pr}{\sin \alpha} = 0 \qquad (2)$$

Equations (1) and (2) are valid for an arbitrarily shaped mandrel and a varying shell thickness. For a conical mandrel, $R_1 = \infty$ and equation (1) becomes

$$\frac{\sigma_\theta}{R_2} = \frac{p}{h} \tag{3}$$

For a shell of constant wall thickness equation (2) becomes

$$\frac{d}{dr}(\sigma_\ell r) - \sigma_\theta - \frac{\mu p r}{h \sin \alpha} = 0 \tag{4}$$

By solving for p from equation (3) and substituting into equation (4) to eliminate p, one obtains

$$\frac{d}{dr}(\sigma_\ell r) - \sigma_\theta - \frac{\mu r \sigma_\theta}{R_2 \sin \alpha} = 0 \tag{5}$$

Since $r = R_2 \cos \alpha$, equation (5) becomes

$$\frac{d}{dr}(\sigma_\ell r) - \sigma_\theta - \frac{\mu \sigma_\theta}{\tan \alpha} = 0 \tag{6}$$

By letting $\mu/\tan \alpha = B$ and combining the last two terms of equation (6) one obtains

$$\frac{d}{dr}(\sigma_\ell r) - \sigma_\theta (1+B) = 0 \tag{7}$$

It is assumed that the element is in a state of essentially plane stress, σ_ℓ and σ_θ being the principal stresses. The two stresses must be related to permit integration of equation (7)

According to the distortion energy condition of plasticity the state of stress is given, for this case, by

$$\sigma_\theta^2 - \sigma_\ell \sigma_\theta + \sigma_\ell^2 = \sigma_o^2 \tag{8}$$

where σ_o is the plastic flow stress. Equation (8) may be solved for σ_θ, with the result

$$\sigma_\theta = \frac{1}{2}\sigma_\ell \pm \frac{1}{2}\sqrt{4\sigma_o^2 - 3\sigma_\ell^2} \tag{9}$$

The positive sign will be used in equation (9) for further development, since for biaxial tension the only region of interest is the first quadrant of the ellipse represented by equation (8).

Upon substitution of equation (9), with the positive sign into equation (7) one has

$$\frac{d}{dr}(\sigma_\ell r) - (1 + B)\left(\frac{1}{2}\sigma_\ell + \frac{1}{2}\sqrt{4\sigma_o^2 - 3\sigma_\ell^2}\right) = 0 \tag{10}$$

or

$$\sigma_\ell + r\frac{d\sigma_\ell}{dr} = \frac{(1+B)}{2}\left(\sigma_\ell + \sqrt{4\sigma_o^2 - 3\sigma_\ell^2}\right) \tag{11}$$

The flow stress, σ_o, is a constant only for an ideally plastic material, but will be considered as a constant here to facilitate integration.

Separation of variables yields

$$\frac{dr}{r} = 2\frac{d\sigma_L}{(B-1)\sigma_L + (B+1)\sqrt{4\sigma_o^2 - 3\sigma_L^2}} \tag{12}$$

Integration of equation (12) yields

$$\ell n\ r = 2\left[\frac{B-1}{4(B^2+B+1)}\ell n\left[(B-1)\sigma_L + (B+1)\sqrt{4\sigma_o^2 - 3\sigma_L^2}\right] + \frac{(B+1)\sqrt{3}}{4(B^2+B+1)}\sin^{-1}\left[\frac{\sqrt{3}}{2}\frac{\sigma_\ell}{\sigma_o}\right]\right] + C \tag{13}$$

The constant of integration will now be evaluated from the condition of no stress before expansion, i.e.

$$\sigma_\ell = 0 \quad @\ r = r \tag{14}$$

In equation (14), r_i is the initial mean radius of the tube. By use of equation (14), it is found that

$$C = \ell n\, r_i - \frac{2(B-1)}{4(B^2+B+1)}\, \ell n\left[2\,(B+1)\,\sigma_o\right] \tag{15}$$

Then equation (13) may be written as

$$\ell n\left(\frac{r}{r_i}\right) = \frac{B-1}{2(B^2+B+1)}\, \ell n\left[\frac{B-1}{2(B+1)}\left(\frac{\sigma_\ell}{\sigma_o}\right) + \sqrt{1-\frac{3}{4}\left(\frac{\sigma_\ell}{\sigma_o}\right)^2}\,\right] + \frac{(B+1)\sqrt{3}}{2(B^2+B+1)}\, \sin^{-1}\left(\frac{\sqrt{3}}{2}\,\frac{\sigma_\ell}{\sigma_o}\right) \tag{16}$$

Equation (16) relates three dimensionless parameters of the tube expansion over a conical mandrel. They are the expansion, r/r_i, the parameter B, a function of the friction coefficient and half-angle of the mandrel, and σ_ℓ/σ_o, a longitudinal stress parameter.

Equation (16) is graphically presented in Figure 2, with σ_ℓ/σ_o and r/r_i being the ordinates and abscissas respectively, with lines of constant B. Figure 2 may be used for the prediction of the performance of a given absorber or for design of an absorber to move under a given load.

This analysis neglects the change in wall thickness as the tube passes over the mandrel as well as the changing flow stress σ_o. If the wall thickness and flow stress were both left in the governing differential equation as variables, analytic solution would probably not be possible. However it is felt that errors introduced by these approximations are not large. On the average the wall thickness decreased about 12 percent on the test absorbers. The average wall thickness was used to compare theory with experiment.

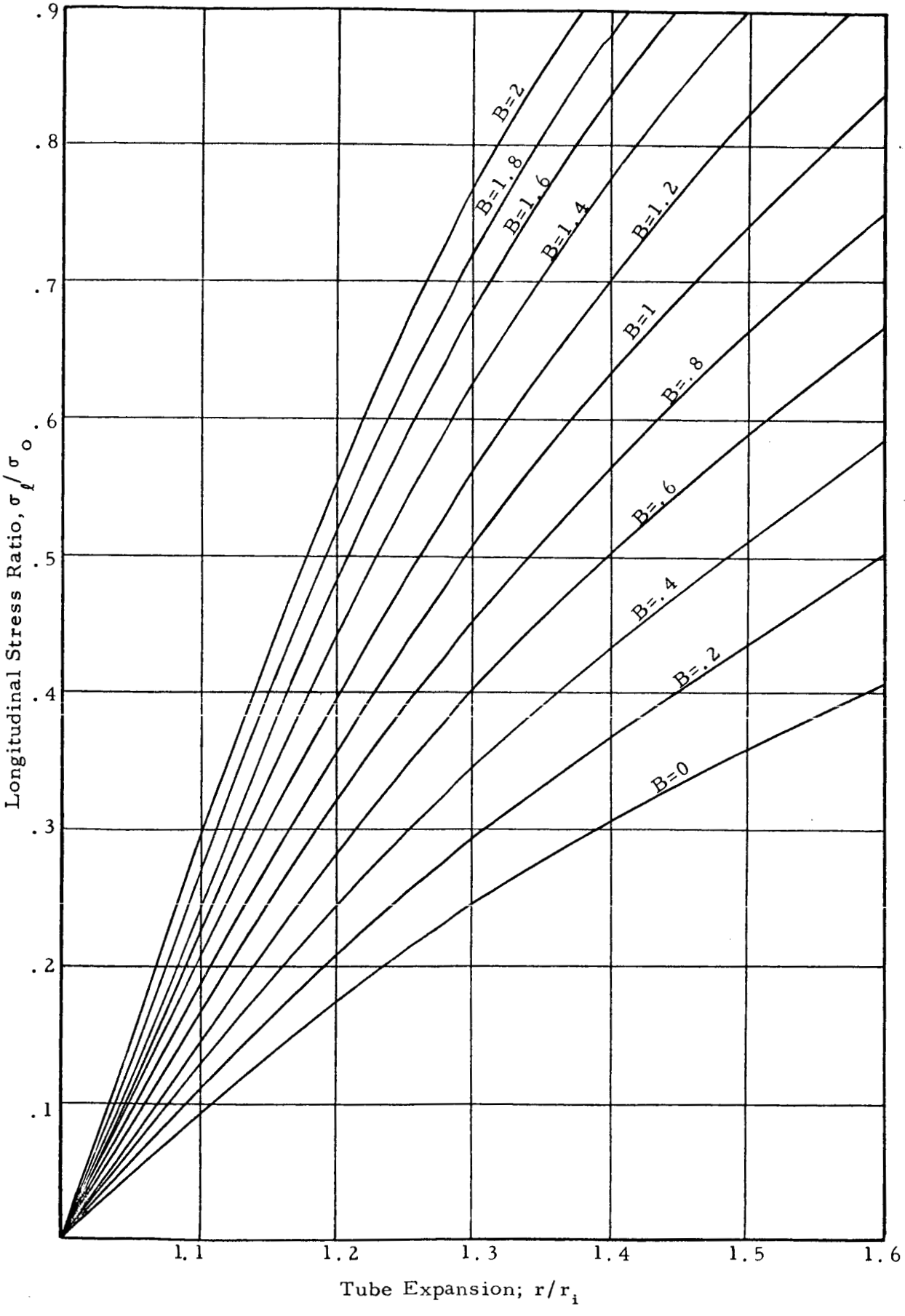

FIGURE 2. TUBE EXPANSION VS LONGITUDINAL STRESS RATIO

III. FRICTION TESTS

Friction tests were performed on quarter sectionsof the 1 1/2 inch O. D. and 1 inch O. D. stainless steel tubing. The apparatus is shown in Figure 3. The hydraulic cylinder exerted a measureable force on the tube section, which was coated with dry film lubricant on both sides, between the two dies. The tensile testing machine was then used to pull the specimen through the dies. A simultaneous reading of hydraulic pressure and tensile load during movement of the specimen yields a coefficient of friction. A formula to correlate these two readings through a friction coefficient will now be developed.

Figure 4 shows a cross section of the specimen and dies. It is assumed that the stresses acting on the specimen consist of a normal stress (or pressure p) and a shearing stress τ. It is assumed that the distribution of these stresses is given by

$$p_i = p_{io} \cos^2 \alpha, \tau_i = p_{io} \sin \alpha \cos \alpha \tag{17}$$

on the concave side of the specimen and by

$$p_o = p_{oo} \cos^2 \alpha, \ \tau_o = p_{oo} \sin \alpha \cos \alpha \tag{18}$$

on the convex side of the specimen.

For equilibrium of the specimen, considering the concave side

$$F = 2 \int_o^\beta p_i r_i Z \cos \alpha \, d\alpha + 2 \int_o^\beta \tau_i r_i Z \sin \alpha \, d\alpha \tag{19}$$

By substituting the expressions for p_i and τ_i from equations (17) into equation (19) and integration of equation (19) one obtains

$$p_{io} = \frac{F}{2 r_i Z \sin \beta} \tag{20}$$

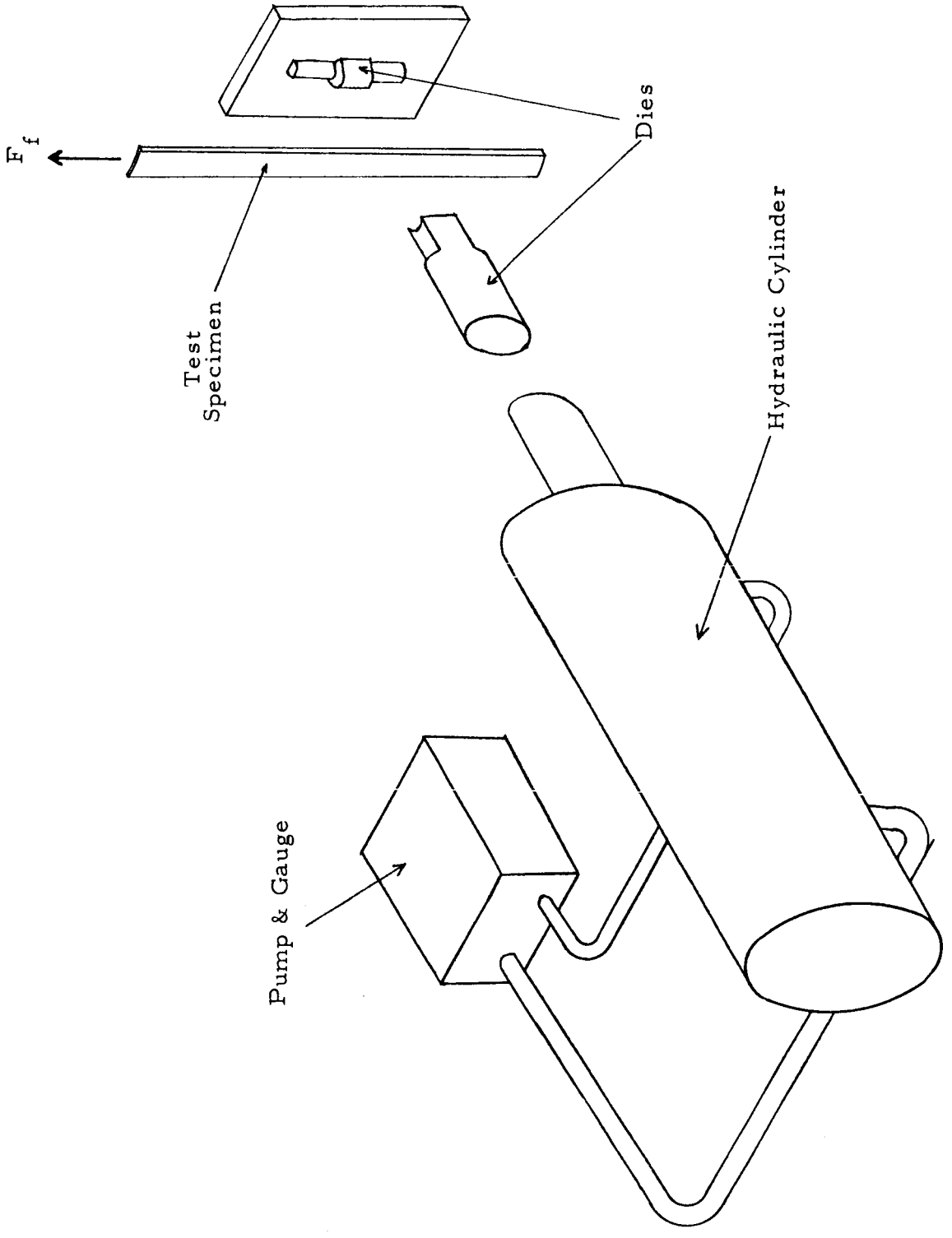

FIGURE 3. FRICTION TESTING APPARATUS

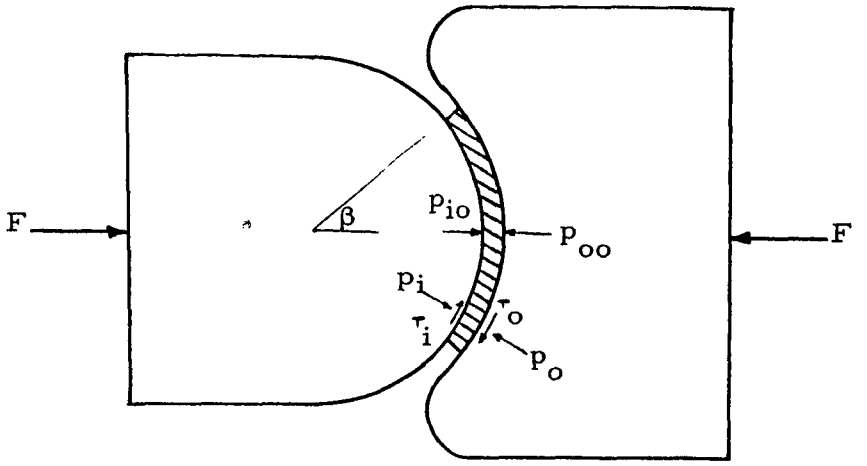

FIGURE 4 FRICTION TEST SPECIMEN AND DIES

In the same manner, considering the convex side of the specimen, one has

$$p_{oo} = \frac{F}{2r_o Z \sin \beta} \tag{21}$$

The normal force between the convex die and the specimen is given by

$$N_i = 2 \int_o^{\beta} (p_{io} \cos^2 \alpha)\, r_i Z d\alpha \tag{22}$$

Integration of equation (22) and substitution of p_{io} from equation (20) yields

$$N_i = \frac{F}{\sin \beta} \left[\frac{1}{2} \beta + \frac{1}{4} \sin 2\beta \right] \tag{23}$$

The same result is obtained for the concave die, and thus the total normal force between dies and the specimen is

$$N = \frac{F}{\sin \beta} \left[\beta + 1/2 \sin 2\beta \right] \tag{24}$$

Then the frictional force, F_f, required to pull the specimen through the dies is

$$F_f = \mu N = \frac{\mu F}{\sin \beta}\left[\beta + 1/2 \sin 2\beta\right] \tag{25}$$

For quarter sections, $\beta = 45°$, and

$$F_f = 1.815 \mu F \tag{26}$$

For a hydraulic cylinder of piston area A,

$$F_f = 1.815 \mu A p' \tag{27}$$

where p' is the hydraulic pressure. If the friction coefficient is independent of pressure between the two surfaces, a linear relation should exist between F_f and p'. Then a friction coefficient, μ, can be calculated from equation (27).

The two best runs are plotted in Figures 5 and 6. Hydraulic pressure was set at each value and the force required to pull the specimen through the dies was measured. At each pressure several readings were taken over a travel of about 1 1/2 inches and averaged to obtain each point in Figures 4 and 5.

Some of the test specimens are shown in Figure 7. There was a tendency to twist and bend passing through the dies near the end of each run. This caused the slight degree of warp near the lower end of the strips, which is most pronounced on specimen C-1. The flaking of the dry lubricant on A-1 and C-1 was caused by seizure of the specimen in the dies at an hydraulic pressure of approximately 1200 psi, resulting in elongation of the strip. Data taken when either of these effects were noticed was discarded. Calculation of μ from equation (27) yields .075 for specimen C-1 and .0865 for specimen D-1.

These values for the friction coefficient are somewhat higher than those

normally associated with dry film lubricants, usually having friction coefficients of approximately .05. However, even slightly higher coefficients are necessary to account for performance of most of the test absorbers.

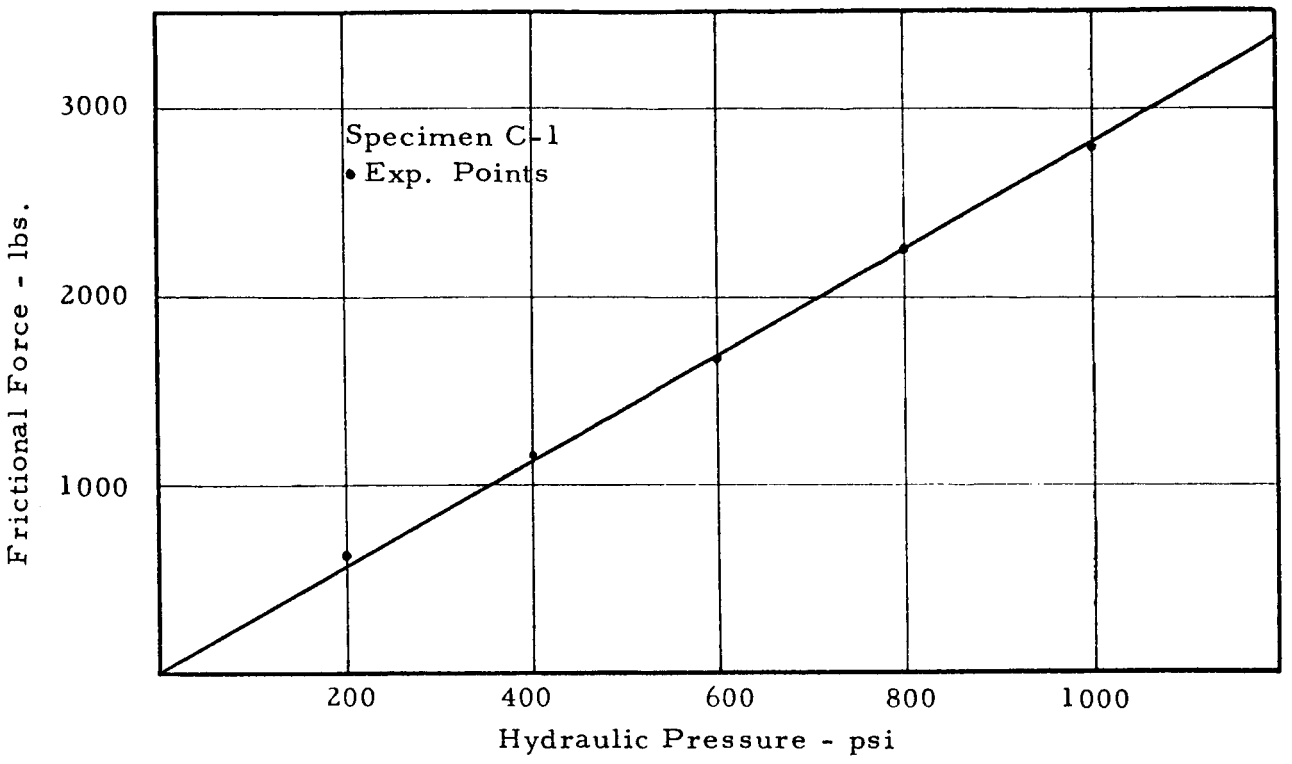

FIGURE 5

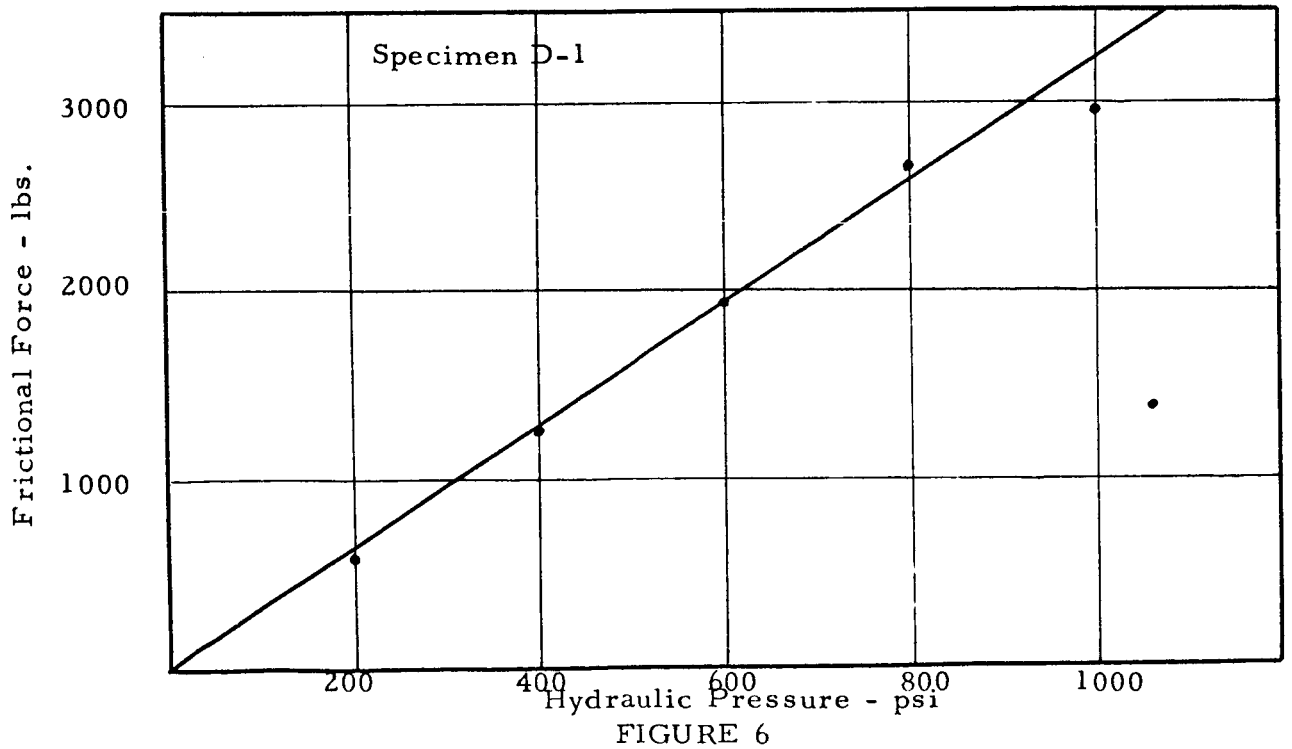

FIGURE 6

FRICTION TEST RESULTS

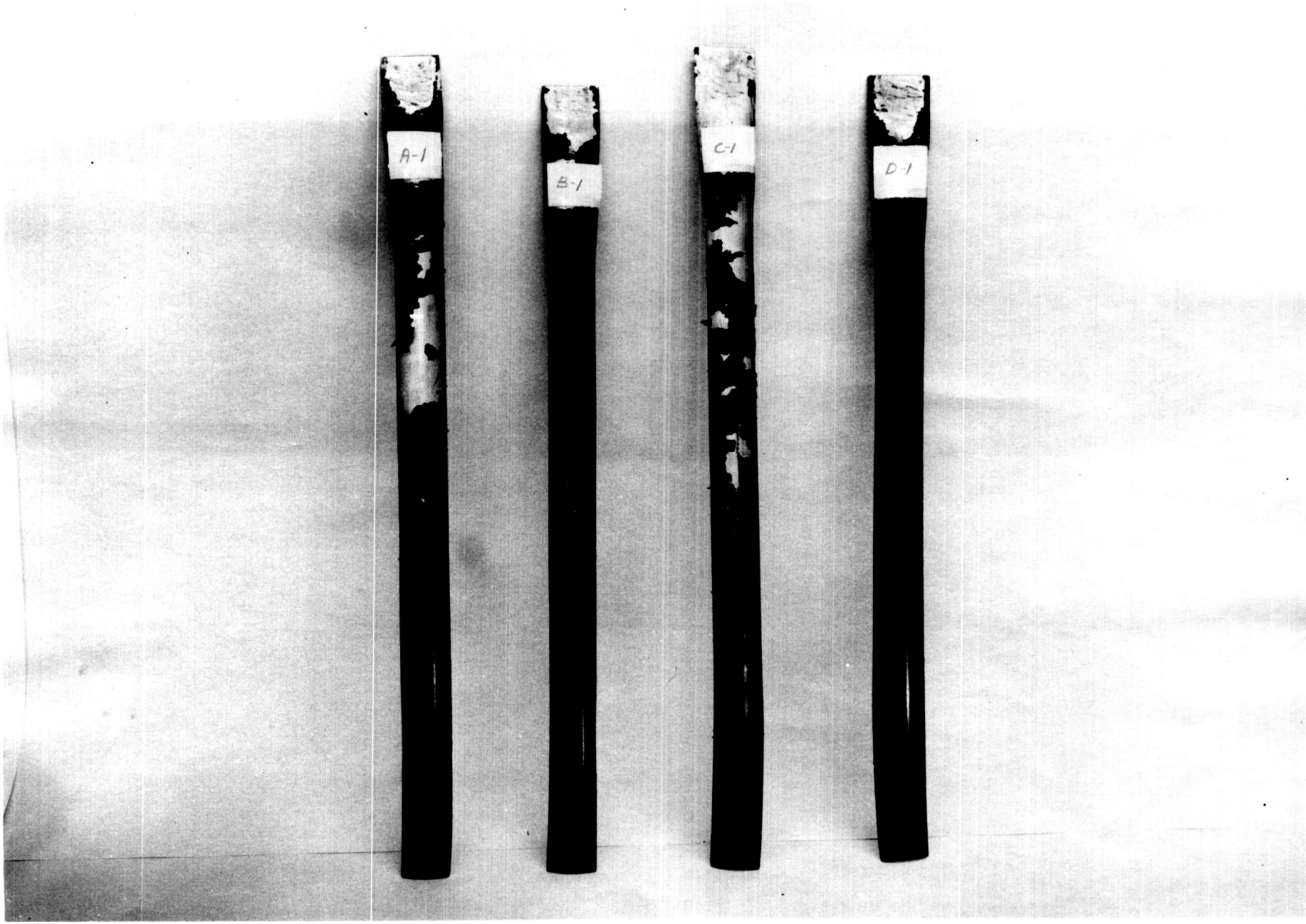

FIGURE 7. FRICTION TEST SPECIMENS (AFTER TESTS)

IV ABSORBER TESTS

Many test absorbers were made and tested. Some had aluminum expansion tubes, but the majority had stainless steel expansion tubes. A typical test absorber is shown in Figure 8.

Early testing was done with mandrels in the shape of a cylinder with the front end rounded. These mandrels gave extremely poor results, the loads varying greatly during the stroke, as well as poor repeatability. This erratic behavior is thought to be primarily due to little contact pressure between the tube and the mandrel after the rounded portion of the mandrel, since loads were consistenly less than anticipated.

This shape was soon discarded in favor of conical mandrels which proved to yield more nearly uniform loads throughout the stroke, as well as lending themselves more readily to analysis. The best results obtained with conical mandrels agree with theory much better than other shapes tested. Also, there is considerable material in the literature concerning tube reducing by means of drawing through conical dies, though none was found concerning tube expansion.

Most of the early tests are omitted in this discussion, since they served only as guides for the development of further tests.

The results of the last two series of tests performed on stainless steel tubes are presented in the form of load-displacement curves. The absorbers were all tested on a Baldwin Universal testing machine with a rate of travel of approximately one inch per minute.

The first group of tests were performed on 2 inch O.D., .095 wall thickness, 304 annealed stainless steel tubing. The mandrel dimensions for both series of tests are given in Table 1.

The load-displacement curves for the first series of tests are given in Figures 10 and 11. These tubes were all internally coated with Electrofilm dry lubricant. It is seen that these tests were somewhat erratic a fairly level curve being obtained only in the test with mandrel number 1. The tests with mandrels number 4, 5, and 6 all display a high starting load and a decreasing load throughout the stroke. The test with mandrel number 3 displayed a similar characteristic, while number 2 behaved in the opposite manner.

Several aluminum tubes were tested at the same time, without lubricant. Also several stainless steel tubes of the same size described above, with some of the same mandrels, were tested without lubricant. The aluminum tubes were much larger than necessary and served only to provide more data for comparison of experiments with theory. Those tubes without lubricant, both aluminum and stainless steel gave extremely erratic load displacement curves, showing that lubrication is necessary for any sort of consistency at all.

The second series of tests, whose results are given in Figures 12, 13, and 14, were performed using 1-1/2 O.D. .065 wall thickness stainless steel. It is noted that the curves for these tests are much more nearly level. Several are perfectly level over a large portion of the stroke.

The fundamental difference between these tests and the previous ones is mandrel length in comparison to tube diameter. In general, the greater the

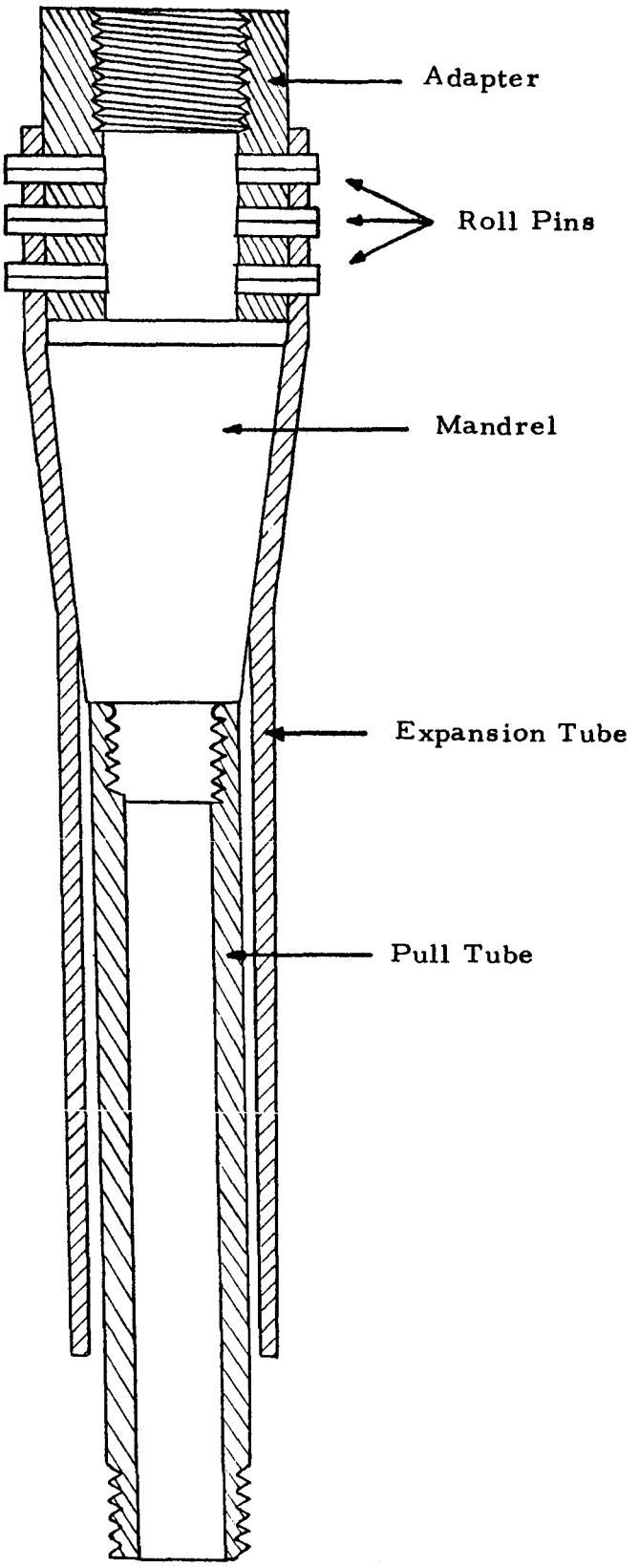

FIGURE 8. TYPICAL TEST ABSORBER

ratio L/D, the more nearly constant the load displacement curve. This may be explained by the fact that localized variations in tube and lubricant properties would have less effect in passing over a long mandrel than a short one, since much more of the tube is in contact with a long mandrel. Longer mandrels, for a given expansion, produce larger loads, due to more friction.

For some unknown reason, probably substandard tube properties, the absorbers with group B mandrels had much lower loads than expected. They had even lower loads than some absorbers with less expansion. All the tubes in the last series of tests were coated with electrofilm at the same time and were baked in a group, so that no appreciable variation in lubricant properties among the tubes should exist.

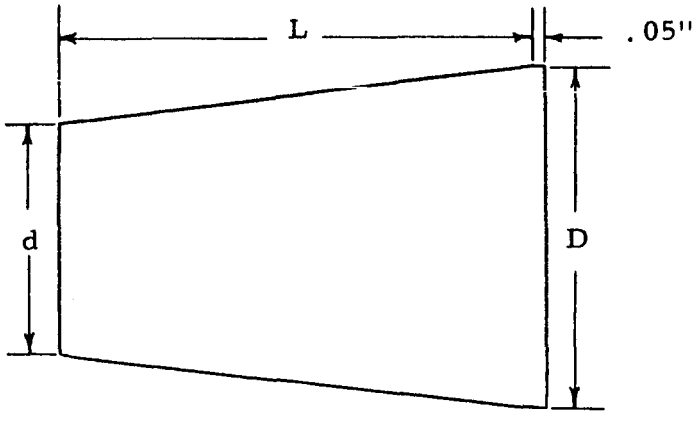

FIGURE 9 BASIC MANDREL DESIGN

2" O.D., .059 Wt.			
No.	D	d	L
1	2.606	1.81	1.488
2	2.606	1.81	2.419
3	2.606	1.81	2.884
4	2.394	1.81	1.902
5	2.534	1.81	1.941
6	2.606	1.81	1.951

1-1/2" O.D., .065 Wt.				
MANDREL GROUP	MANDREL NO.	DIMENSIONS		
		D	d	L
A	29	1.666	1.25	2.04
	59	1.6645	1.249	2.76
	89	1.664	1.250	3.435
B	19	1.7675	1.249	1.91
	49	1.7684	1.249	2.53
	79	1.7675	1.251	3.18
C	9	1.868	1.248	1.82
	39	1.869	1.250	2.425
	69	1.865	1.250	3.05

TABLE 1. MANDREL DIMENSIONS

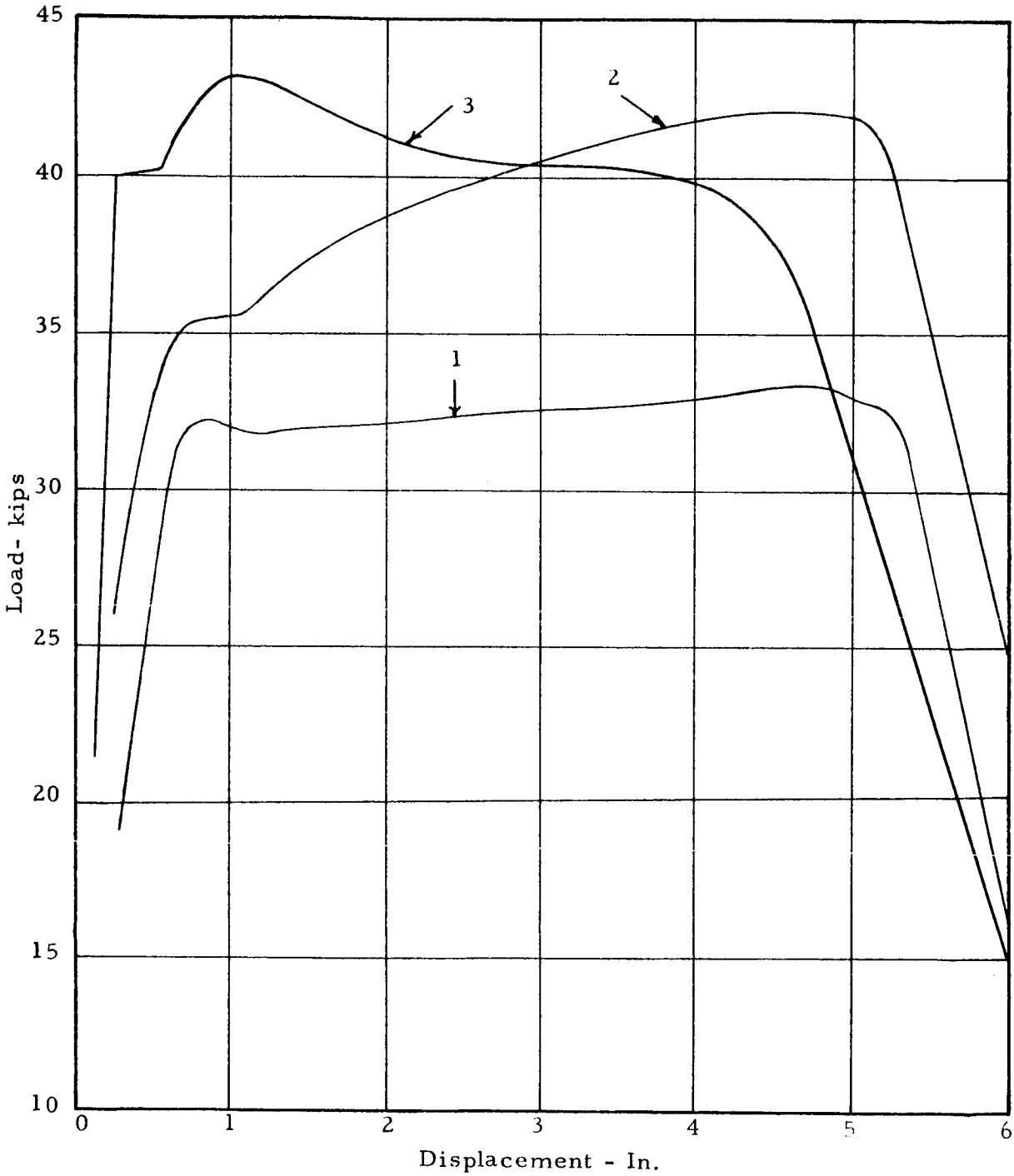

FIGURE 10. LOAD VS DISPLACEMENT

ABSORBERS 1, 2, AND 3

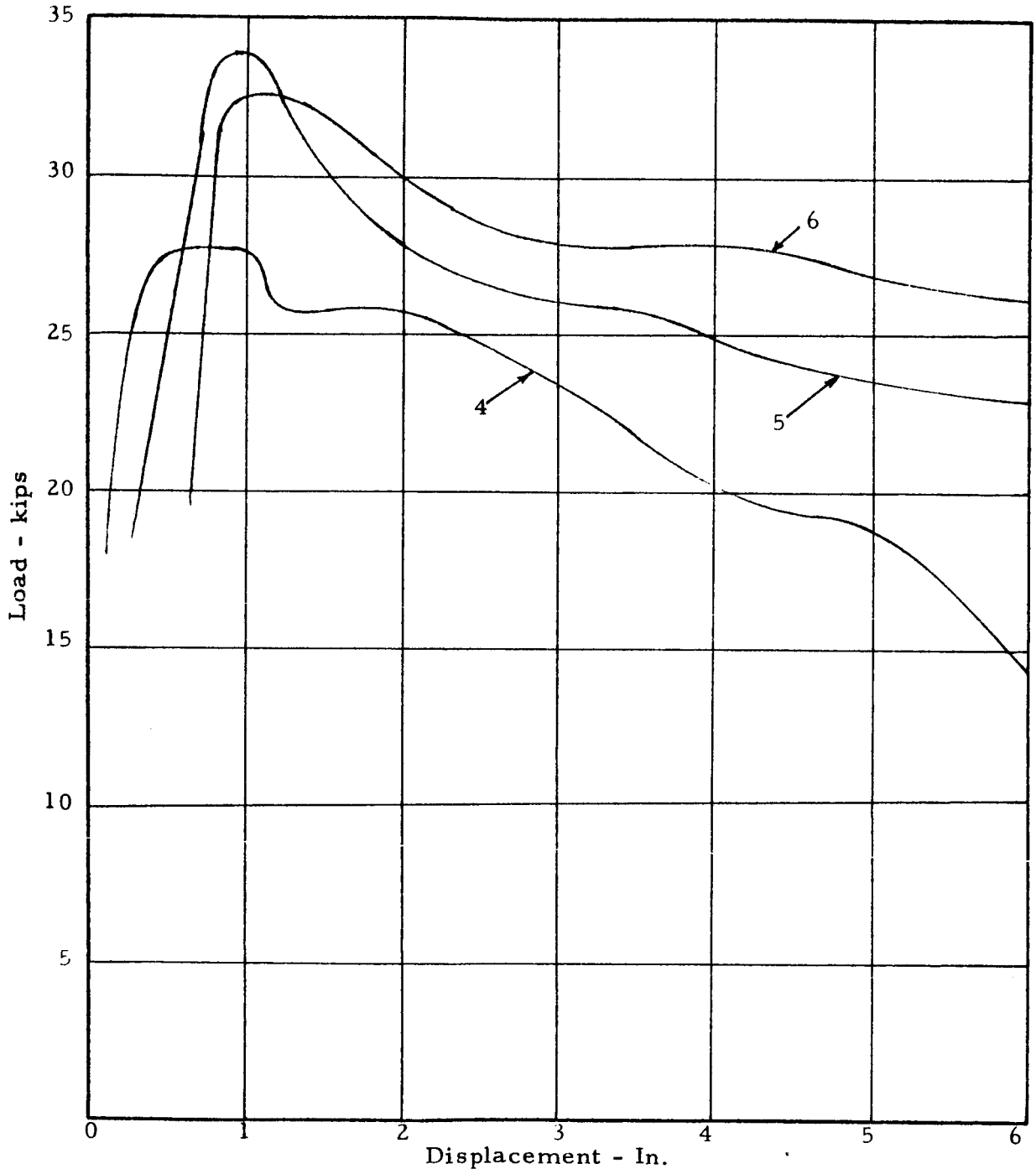

FIGURE 11. LOAD VS DISPLACEMENT, ABSORBERS 4, 5, and 6

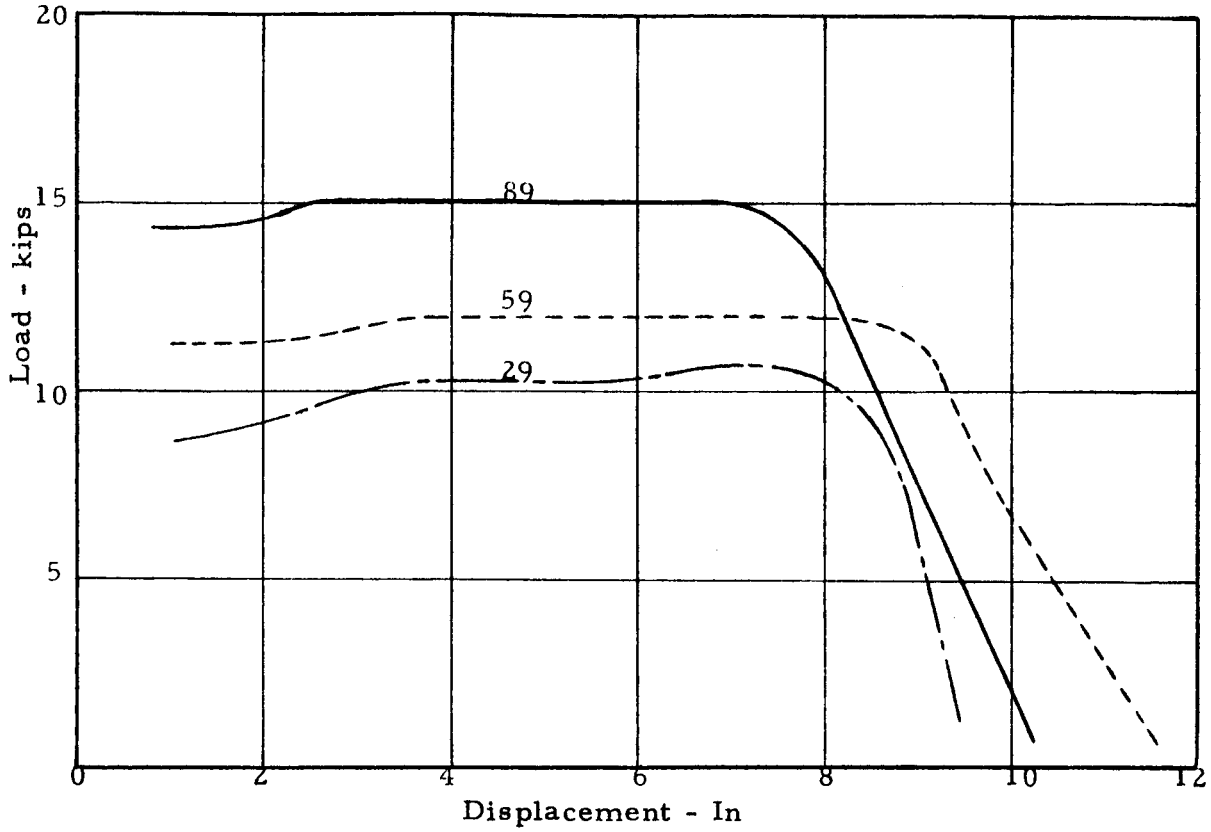

FIGURE 12. LOAD VS DISPLACEMENT, GROUP A

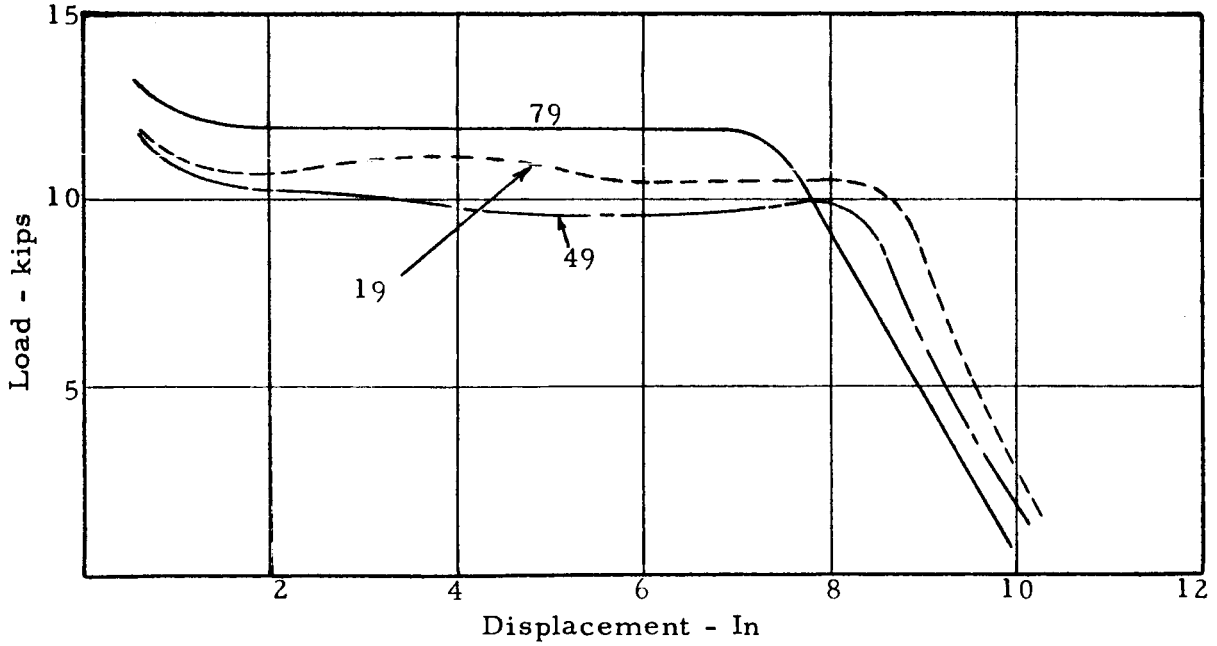

FIGURE 13. LOAD VS DISPLACEMENT, GROUP B

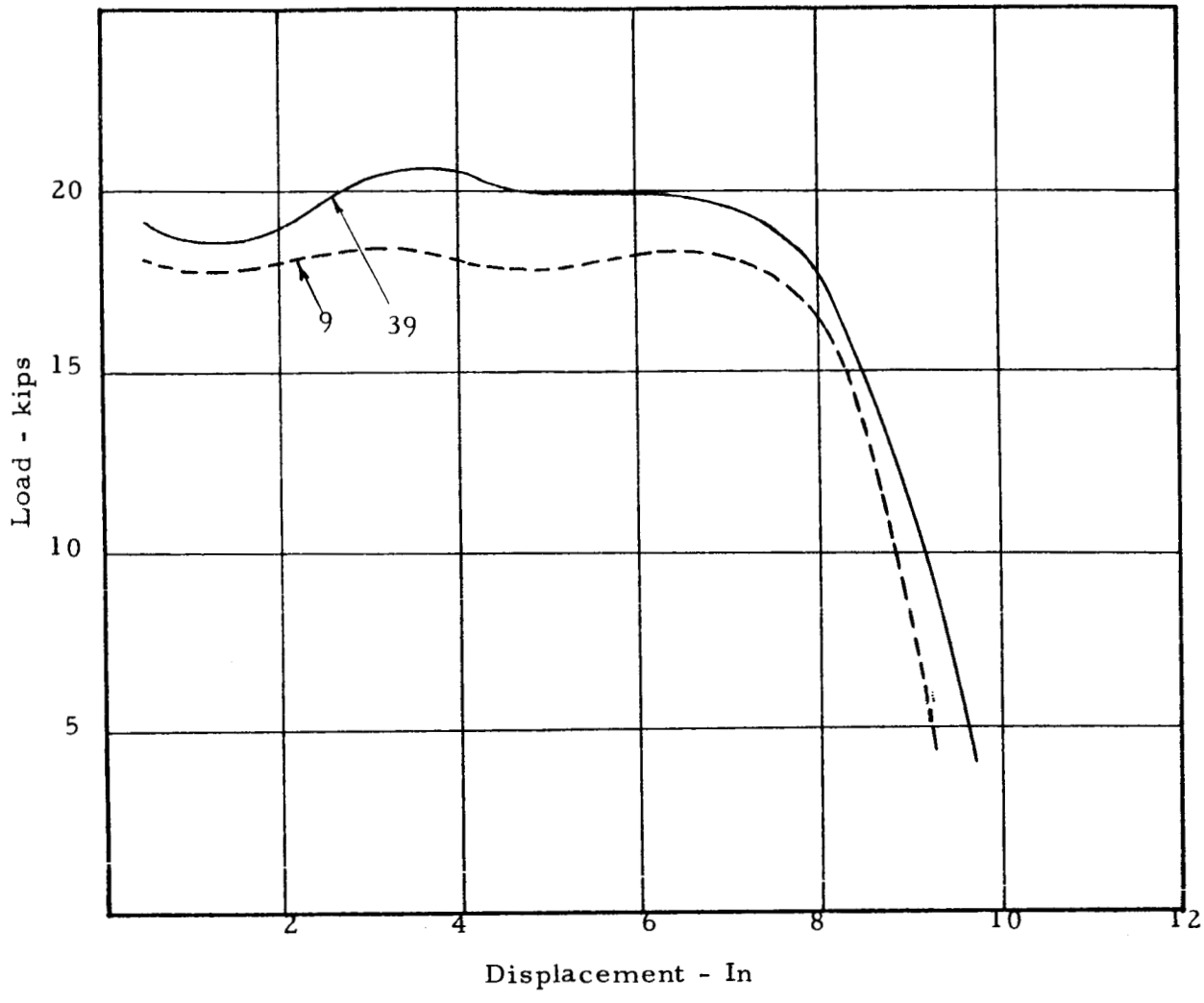

FIGURE 14. LOAD VS DISPLACEMENT, GROUP C

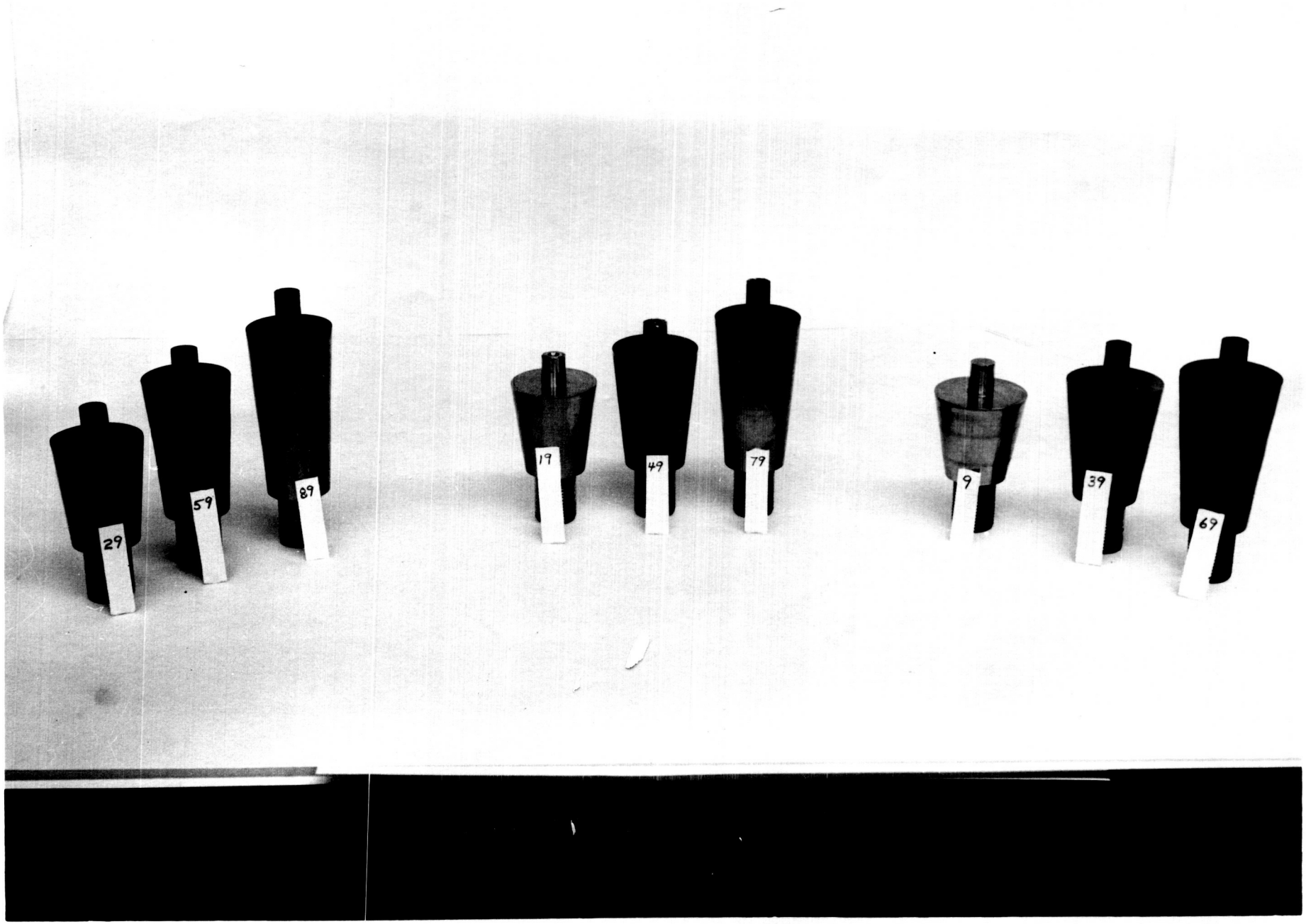

FIGURE 15. GROUPS A, B, AND C MANDRELS

V. AGREEMENT WITH THEORY

The results of the analysis presented in Section 1 will now be compared with the test results given in Figures 10, through 14. The consistency of the friction coefficient necessary to make theory and test results agree is the most convenient criterion for comparison. The method of obtaining the calculated friction coefficient will be carried out for the absorber with mandrel number 59, and the results given for the rest. These will then be compared with experimental friction coefficient information.

The absorber with mandrel number 59 required 12,000 pounds pull for steady movements. The measured wall thickness before expansion was .066 and .0565 after expansion. The mandrel, of 1.6645 inches large diameter caused an average circumferential strain of .201 in/in. From the true stress-strain curve, Figure 16, σ_o = 87 ksi. The following equation relates the stress ratio, σ_ℓ/σ_o, at the end of the mandrel to the pull load.

$$P = A_f \frac{\sigma_\ell}{\sigma_o} \sigma_o \cos \alpha \qquad (28)$$

Using P = 12,000 pounds, σ_o = 87 ksi, α = 4 degrees, 23' and A_f = .332 in^2, one obtains

$$\frac{\sigma_\ell}{\sigma_o} = .416$$

Referring to Figure 14, at σ_ℓ / σ_o = .416 and r/r_i = .2, one obtains B = 1.3. Then since

$$\mu = B \tan \alpha$$

$$\mu = (1.3)(.07666) = .0995$$

A value of .0995 is thus obtained for the friction coefficient. The friction coefficients obtained in this manner are given in Table 2. Where no steady pull load existed, an average load from the center five inches of travel was used.

1	2	3	4	5	6
.051	.071	.055	.025	0	0
Group A		Group B		Group C	
29 59 89		19 49 79		9 69 39	
.107 .0995 .113		.053 .029 .045		.117 - .104	

TABLE 2. CALCULATED FRICTION COEFFICIENTS

Calculated coefficients for the large aluminum tube. Absorbers previously mentioned are .0975, .0815, and .107 with lubricant, and .342, .267, and .338 without lubricant. Three stainless steel tubes identical to those in the first series, used without lubricant had calculated coefficients of .124, .147, and .124. Two smaller stainless steel tubes not previously mentioned both yeilded coefficients of .101.

Inspection of the calculated friction coefficients shows that for lubricated tubes a coefficient in the range .09-.11 seems to be most reliable since most of the tests indicate a coefficient in this range, for lubricated tubes.

The coefficients obtained with no lubricant agree fairly well with those given in handbooks.

The information gained from the last series of tests was used in the

final mandrel design, since these were the most consistent, both in uniformity of load during the stroke, and in calculated friction coefficients, with the exception of group B.

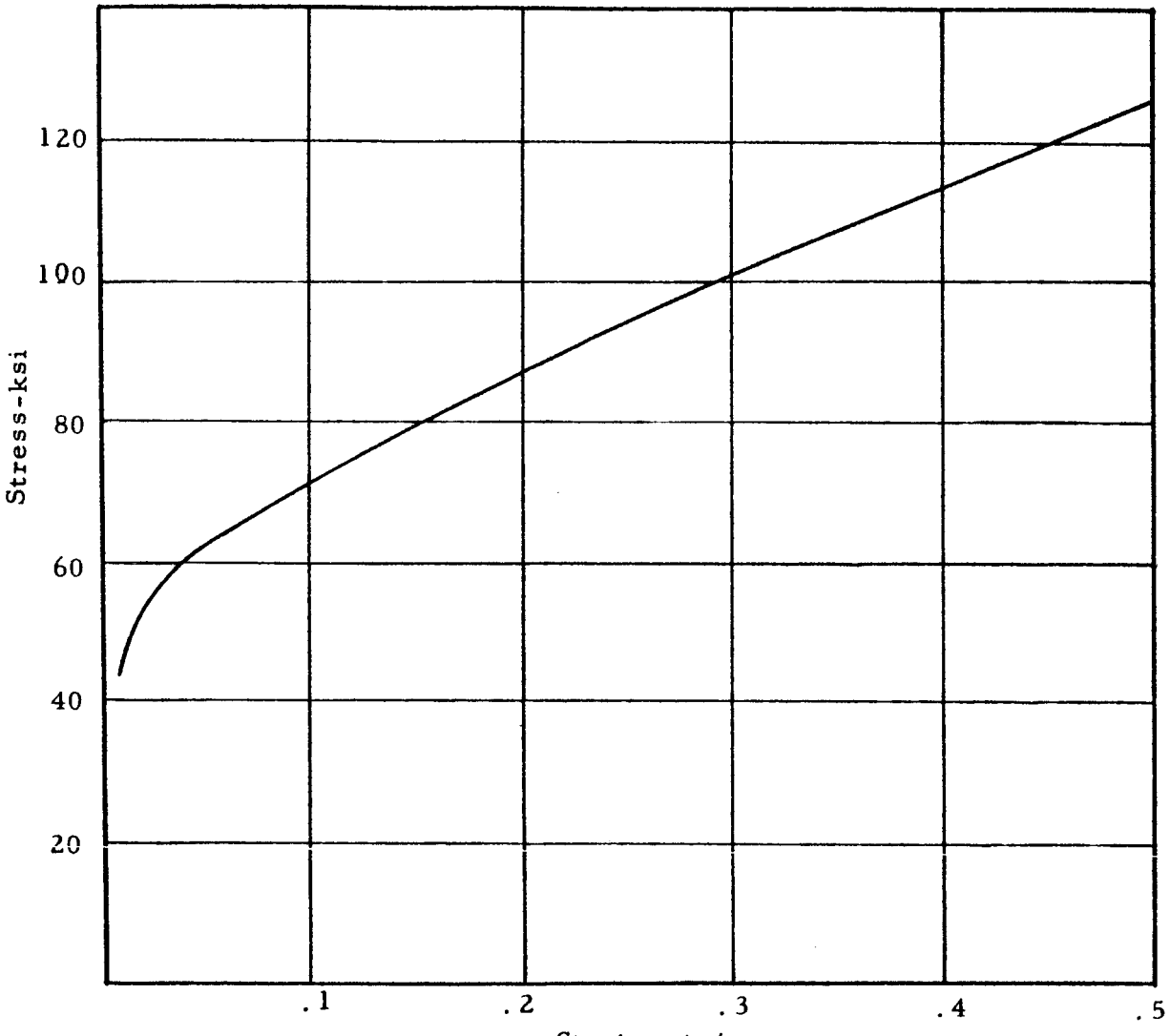

FIGURE 16. TRUE STRESS-STRAIN CURVE
304 S.S., Annealed

VI. MANDREL DESIGN

From the test result of the number 39 mandrel, which had a pull load very close to 20,000 pounds, a mandrel slightly longer, with the same tube expansion was designed. The calculated friction coefficient for the number 39 mandrel was used in the design. The mandrel dimensions to yield a 20,000 pounds absorber with the .065 wall thickness, 1 1/2 O.D. 304 stainless steel tubing are shown below.

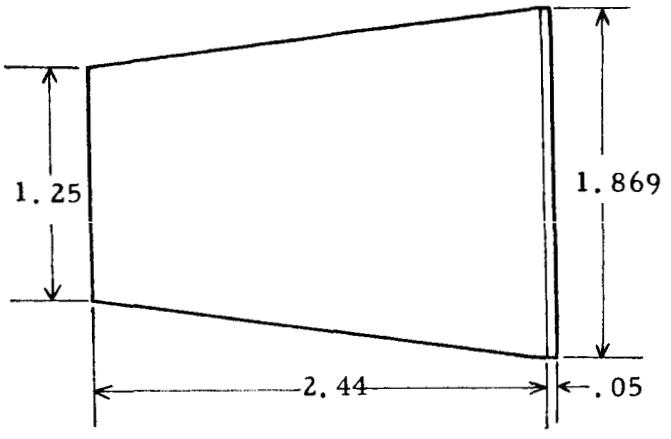

FIGURE 17. MANDREL DESIGN

VII. PROBLEM AREAS

The dry film lubricant seems to be somewhat erratic in its lubricating ability. This was shown by the differences in friction tests. Also the variation of friction coefficients needed to correlate the analysis with absorber tests. Part of this discrepancy is undoubtly due to the approximate character of the analysis, but it is not felt to be the major part. The friction coefficient's dependence on the velocity of the sliding surfaces, if any, should be investigated. This should be taken into account in the study of dynamic behavior of the absorbers.

The absorbers delivered to NASA showed no large deviations in load characteristics when dynamically tested than when quasi-statically pulled at Hayes. The loads tended to be slightly lower, indicating a possible slight decrease of friction coefficient with velocity.

An as yet unexplained vibration existed when most of the absorbers were dynamically tested at NASA. This is not a characteristic solely of this type absorber, for another type tested by NASA displayed the same phenomenon.

Many absorbers required a load slightly higher than the steady pulling load to begin movement. Possible elimination of this undesirable characteristic by annealing the expansion tube after the expansion necessary to position the mandrel, or by other means such as reducing the wall thickness at the beginning of the stroke, should be studied.